Int. J. Electrochem. Sci., 15 **(2020)** 4072 – 4088, doi: 10.20964/2020.05.42

International Journal of ELECTROCHEMICAL SCIENCE
www.electrochemsci.org

Dielectric and Optical properties of $RE_{1.8}Sr_{0.2}CuO_{4\pm\delta}$ (RE = La, Pr, Nd)

Basma Marzougui[1,2], Mohamed Ikbal Houchati[1], Youssef Ben Smida[1,], Naser Sdiri[3], Riadh Marzouki[4,5], Ahmed Hicham Hamzaoui[1]*

[1] Université de Carthage, Centre National des Recherches en Sciences des Matériaux, Laboratoire de Valorisation des Matériaux Utiles, Technopôle Borj Cedria, B.P. 73, 8027 Soliman, Tunisie
[2] Université de Carthage, Faculté des sciences de Bizerte, Jarzouna - Bizerte – 7021, Tunisie.
[3] Université de Carthage, Centre National de Recherches en Sciences des Matériaux, Laboratoire de Physicochimie de Matériaux et leurs Applications, Technopôle Borj Cedria, BP 73, 8027 Soliman, Tunisie.
[4] Department of Chemistry, College of Science, King Khalid University, Abha 61413, Saudi Arabia.
[5] Department of Chemistry, Faculty of Sciences of Sfax, University of Sfax, 3038, Tunisia
[*]E-mail : youssef_smida@yahoo.fr

Received: 9 December 2019 / *Accepted:* 30 January 2020 / *Published:* 10 April 2020

The present work investigates the optical and dielectric properties of three Sr-doped rare earth copper oxide $RE_{1.8}Sr_{0.2}CuO_{4\pm\delta}$ (RE=La, Nd, Pr) synthesized by the solid-state reaction at 1000 °C. The title samples were characterized by X-ray powder diffraction which shows that the three samples crystallize in the tetragonal system with close unite cell parameters. The morphology and the practical size of the powder were studied by the means of Scanning Electron Microscopy and the grain size are about 1-5µm. The optical band gap of the titled compounds have been determined and they are in the 1.19-1.30 eV range. Detailed studies of dielectric properties of the compounds as a function of frequencies at different temperatures (270-500°C) show that $La_{1.8}Sr_{0.2}CuO_{4\pm\delta}$ and $Pr_{1.8}Sr_{0.2}CuO_{4\pm\delta}$ have a very high dielectric constant $\varepsilon' > 10^9$ compared to $Nd_{1.8}Sr_{0.2}CuO_{4\pm\delta}$ ($\varepsilon' \approx 800$). While $La_{1.8}Sr_{0.2}CuO_{4\pm\delta}$ and $Pr_{1.8}Sr_{0.2}CuO_{4\pm\delta}$ have an important dielectric loss (≈ 65-70) compared to $Nd_{1.8}Sr_{0.2}CuO_{4\pm\delta}$ which has a very low value (≈ 0.65).

Keywords: Cuprate, Rare Earth, optical bond gap, dielectric properties.

1. INTRODUCTION

The copper oxides $RE_{2-x}Sr_xCuO_{4\pm\delta}$ (RE= rare earth) have been a subject of intensive studies [1] since the discovery of superconductivity of cuprate $Nd_{1.85}Ce_{0.15}CuO_{4\pm\delta}$ [2-4]. From a crystallography point of view, the cuprate materials RE_2CuO_4 (RE = rare earth) have a richness of structural properties

[5-7]. In fact, the ionic radii of rare earth elements of copper oxides RE_2CuO_4 (RE = rare earth) is an essential criterion which imposes the type of structure adopted by the material. Indeed, the cuprate La_2CuO_4 may crystallize at low temperature in two systems: the orthorhombic system with space group *Bmab* that usually named LTO (low temperature orthorhombic) phase and in the tetragonal system with space group *I4/mmm* which is called LTT (low temperature tetragonal) phase or simply T-phase [8]. The obtaining of LTT phase or LTO depends on the method of synthesis. The other lanthanum copper oxides RE_2CuO_4 (RE = rare earth) crystallize at low temperature in the tetragonal system, space group *I4/mmm* and their structures were usually named T'-phase. The difference between T-phase and T'-phase is related to the position of an oxygen which is on 4e Wyckoff position in T-phase and on 4d Wyckoff position in T'-phase [9].

The lanthanum copper oxide La_2CuO_4 shows a colossal dielectric constant ε_r' in the 10^3-10^4 range displayed over the 1Hz-1MHz frequency range and the -100-150°C temperature range [10]. The dielectric constant of $La_{1.95}Sr_{0.05}CuO_{4\pm\delta}$ is about 2.10^5 at 4.2K (0.1 to 10kHz) which was much larger than that of La_2CuO_4 [11]. The dielectric constant increase was explained by the increase of the hole concentration in the sample [11]. The substitution allows also to decrease the temperature of relaxation from 34.2 K to 4.2K [11]. For the Europium copper oxide Eu_2CuO_4, the dielectric constant was about of 10^3-10^4 for coarse grain and 10^4-10^5 for fine grained in the frequency range of 1kHz-1MHz and the in temperature range of 173K-423K [12]. This result proves the effect of the microstructure on the dielectric properties.

The dielectric properties of $Nd_{2-x}Sr_xCuO_{4\pm\delta}$ (x=0; 0.05; 0.10; 0.15; 0.20) have been studied at room temperature in the 50Hz-5MHz frequency range [13]. The parent compound Nd_2CuO_4 shows the highest dielectric constant value [13]. The introduction of Sr^{2+} in the structure allows decrease in the dielectric constant thus ergo the samples $Nd_{1.8}Sr_{0.2}CuO_{4\pm\delta}$ having the lowest value [13]. The dielectric study of the copper oxide Pr_2CuO_4 in the frequency 0.1Hz-1MHz and -100-150°C temperature range showed that the material exhibits a large colossal dielectric constant ε_r' of about 10^4. The dielectric loss (tanδ) of Pr_2CuO_4 in the same ranges is between 0.1 and 5 [14]. The dielectric properties of other rare earth copper oxides such as Gd_2CuO_4 [15], Eu_2CuO_4 [12] and Sm_2CuO_4 [16] have been studied. For the Gd_2CuO_4 oxide, the dielectric constant was measured in the 20 Hz- 1MHz frequency range and in the 20 K-300K temperature range. The sample shows a very high real part ε_r'>10^4 at 300 K. The ε"(T) and D(T) curves both show a relationship frequency dependence, the first being related to the antiferromagnetic transition at T=230K and the second was related to the change of conduction mechanism [12].

The optical properties of the rare earth copper oxide RE_2CuO_4 (RE= rare earth) interested several researchers for using them in photocatalytic reactions. In fact, the optical bond gap should be quite large to support the dissection energy of water which was about 1.23 eV. On the other hand, the optical bond gap should be smaller than 2.1 eV [17], which would allow materials to capture and collect most of solar energy. In this aim, the optical properties of serval RE_2CuO_4 oxide have been determined. For example, La_2CuO_4 shows a broad absorption bond in Uv-vis region [200-800 nm] with a bond gap of about 1.24 eV [17] which was attributed to the charge transfer interaction $O^{2-}\rightarrow Cu^{2+}$. For the RE_2CuO_4 (RE=Pr, Nd, Sm, Gd), the optical bond gap determined from nonmetric crystallite size are 0.79 eV, 1.06 eV, 1.20 eV and 1.36 eV respectively [18]. The variation of the optical band gap has been correlated to the ionic radii of the rare earth element [18] and it has been shown that the band gap decrease with the increase

of the ionic radii. The optical properties of doped lanthanum copper oxide $La_{2-x}M_xCuO_{4-y}$ (M=Ca, Sr and Ba) were the subject of some papers [19-21]. The authors take into account the effect of the grain size on the optical properties of prepared samples, thus they have used soft chemistry synthesis methods such sol-gel, combustion and co-precipitation [19-21]. It can be seen that the optical band gap decreases with the increase of the rate of Ca^{2+} and Ba^{2+}, however it increases conversely in the case of Sr^{2+}. For the undoped La_2CuO_4 the authors cited the same value of optical bond gap, which was about of 1.88 eV [19-21]. This value is different to the value quoted by references [17] and this is probably due to the grain size of crystallite.

The idea of this paper is to study the effect of rare earth on the optical and dielectric properties of $RE_{1.8}Sr_{0.2}CuO_{4\pm\delta}$ (RE=La, Pr, Nd). The manuscript is composed of three parts: The first part of the paper is devoted to the synthesis of title samples by solid-state reactions. The purity of the powder and unit cell parameters are carried out by the means of the XRPD technique. The homogeneity, grain size and crystallite morphology are determined by using the scanning electron microscopy technique. The second part of the paper is dedicated to the optical properties of the title samples and the determination of the optical bond gap followed by a discussion and comparison with previous work. The last part is conserved for the dielectric properties of the $RE_{1.8}Sr_{0.2}CuO_{4\pm\delta}$ (RE=La, Pr, Nd) oxides.

2. EXPERIMENTAL SECTION

The title compounds have been prepared by using the solid state method. The following oxides La_2O_3 (Alfa Aeser, 99.99 %), Nd_2O_3 (Alfa Aeser, 99.99 %), Pr_6O_{11} (Aldrich, 99.9 %), CuO (Alfa Aeser, 99.7 %) and $SrCO_3$ (Aldrich, 99.9 %) have been used as starting reagents. Lanthanum oxide La_2O_3 was heated at 900 °C for one night before weighing the reagent. The powders were mixed in stoichiometric quantities and then grounded in an agate mortar and were heated at 900 °C for 12h, then at 1000 °C for 24 hours.

The purity of prepared samples was confirmed by X-ray powder diffraction by using Bruker D8 Advance diffractometer equipped with a Cu anticathode (CuKα radiation λ=1.54056 Å) at room temperature. The XRD measurements were performed under Bragg–Brentano geometry in the 10°-80° range with step 0.02°.

UV-Vis-DRS spectra were measured in absorbance mode on a Perkin Elmer Lambda 35 at room temperature. The wavelength range is from 200 nm to 2500 nm with a step width of 10 nm.

The scanning electron microscopy was used to determine the morphology and size of grains of the prepared powders. The micrographs were carried out by using the JSM 6301 microscopy.

The impedance measurements were carried out using an impedance analyzer Solartron 1260 in the 10Hz to 13MHz frequency range. The samples were compacted as pellets by using a uniaxial press. Two platinum (Pt) electrodes were fixed on both sides of each pellet by applying a layer of silver paste to ensure good electrical contact. Before the measurements, the samples were heated at 150° C for 12 hours to remove traces of water in the pores of the pellet.

3. RESULTS AND DISCUSSION

3.1. XRD powder analysis

In agreement with the literature, the incorporation of Sr in the RE_2CuO_4 (RE = La, Pr, Nd) materials may occur a phase transition from tetragonal to orthorhombic system and vice versa [9]. In fact, the $La_{2-x}Sr_xCuO_{4\pm\delta}$ materials change the crystallographic system from orthorhombic to tetragonal when the strontium concentration reaches 10%.

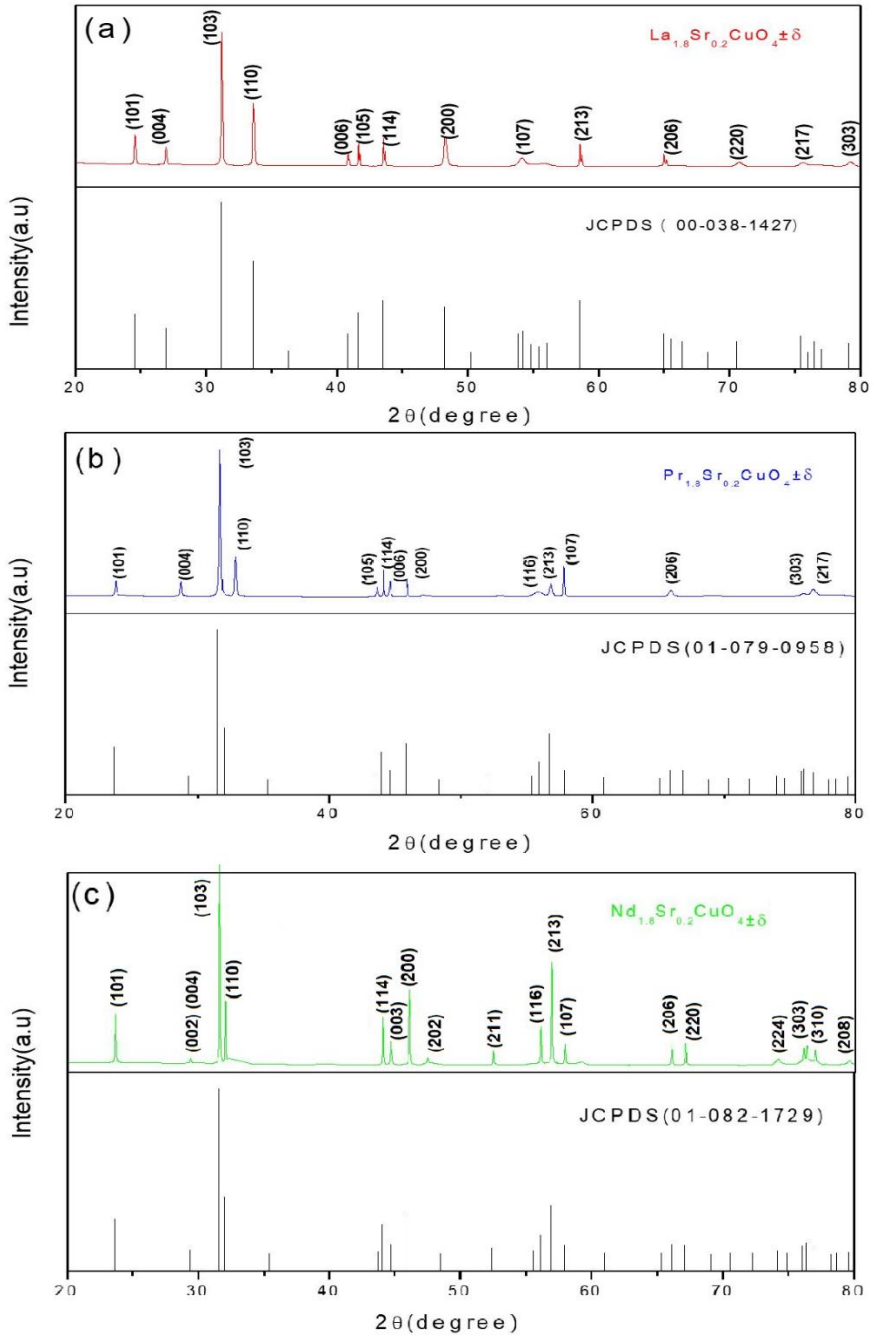

Figure 1. XRD powder patterns of **(a)** $La_{1.8}Sr_{0.2}CuO_{4\pm\delta}$, **(b)** $Nd_{1.8}Sr_{0.2}CuO_{4\pm\delta}$ and **(c)** $Pr_{1.8}Sr_{0.2}CuO_{4\pm\delta}$, with the JCPDS numbers of references patterns.

For $RE_{1.8}Sr_{0.2}CuO_{4\pm\delta}$ (RE=La, Pr and Nd), all peaks were indexed in the tetragonal system with space group (*I4/mmm*) (Figure 1) and no additional pics are observed. The unit cell parameters are obtained by using the DICVOL program included in X'Pert High Score Plus package. The unit cell parameters of $RE_{1.8}Sr_{0.2}CuO_{4\pm\delta}$ (RE=La, Pr, Nd) are regrouped in Table 1**.**

Table 1. The unit cell parameters of $RE_{1.8}Sr_{0.2}CuO_{4\pm\delta}$ (RE=La, Pr, Nd)

Samples	a(Å)	b(Å)	c(Å)	V(Å^3)
$La_{1.8}Sr_{0.2}CuO_{4\pm\delta}$	3.769(1)	3.769(1)	13.26 (1)	188.31(2)
$Pr_{1.8}Sr_{0.2}CuO_{4\pm\delta}$	3.944(8)	3.944(8)	12.210(3)	189.95(2)
$Nd_{1.8}Sr_{0.2}CuO_{4\pm\delta}$	3.942(5)	3.942(5)	12.167(5)	189.07(2)

3.2. Microstructural study

Two methods are used to study the microstructure of the samples. The calculation of the crystallite size by using the Debye-Scherrer equation [22]:

$$D=\frac{0.9*\lambda}{\beta*\cos\theta} \quad (1)$$

Where, λ is the wavelength of the X-ray (λ=1.54 Å for CuKα), β is the broadening of the diffraction line measured at half of its maximum intensity (FWHM: full width at half maximum), θ is the Bragg's diffraction angle and D is the crystallite size.

The calculated crystallite size of the title samples are shown in Table 2. The average crystallite size of $RE_{1.8}Sr_{0.2}CuO_{4\pm\delta}$ (RE=La, Pr, Nd) are varied between 70 nm and 124 nm.

Table 2. The calculated crystallite size of $RE_{1.8}Sr_{0.2}CuO_{4\pm\delta}$ (RE=La, Pr, Nd) using the Debye-Scherrer equation

Samples	2θ (deg)	(hkl)	FWHM (β radian)	crystallite size (nm)
$La_{1.8}Sr_{0.2}CuO_{4\pm\delta}$	31.1562	103	0.00137	105.02
$Pr_{1.8}Sr_{0.2}CuO_{4\pm\delta}$	31.7020	103	0.00204	70.63
$Nd_{1.8}Sr_{0.2}CuO_{4\pm\delta}$	31.6429	103	0.00116	124.18

The second method is by using the scanning electron microscopy to determine the grain size and morphology. The scanning electron microphotographs (SEM) of $RE_{1.8}Sr_{0.2}CuO_{4\pm\delta}$ samples are displayed in Figure 2.

The examination of the micrographs makes it possible to deduce some remarks. First, the powders consist of homogeneous and almost identical particles. They are basically spherical in shape. The particles are well connected with each other and formed well-bonded porous network. Second, the average size of the particles of $Nd_{1.8}Sr_{0.2}CuO_{4\pm\delta}$ is about of 700 nm, 2 μm for $Pr_{1.8}Sr_{0.2}CuO_{4\pm\delta}$ and 1.5 μm for $La_{1.8}Sr_{0.2}CuO_{4\pm\delta}$. We can show also the formation of hard agglomeration for $La_{1.8}Sr_{0.2}CuO_{4\pm\delta}$ and $Nd_{1.8}Sr_{0.2}CuO_{4\pm\delta}$ compared to $Pr_{1.8}Sr_{0.2}CuO_{4\pm\delta}$.

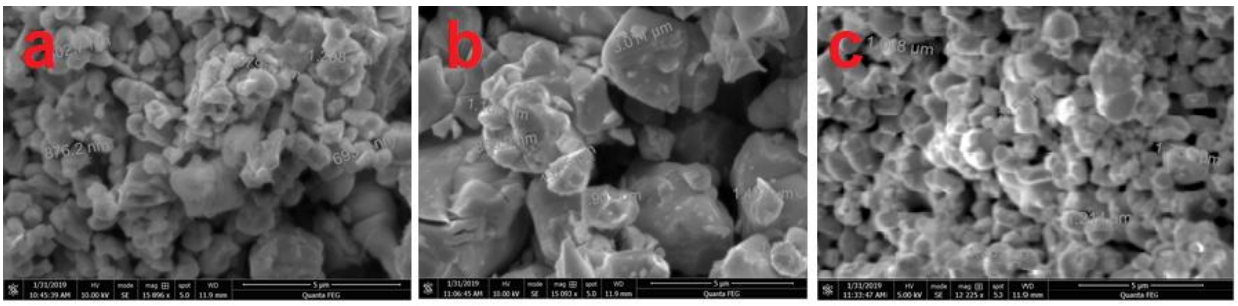

Figure 2. The microphotographs (SEM) of (a) $La_{1.8}Sr_{0.2}CuO_{4\pm\delta}$, (b) $Pr_{1.8}Sr_{0.2}CuO_{4\pm\delta}$ and (c) $Nd_{1.8}Sr_{0.2}CuO_{4\pm\delta}$.

3.3. Optical Properties

Figure 3 (a&b) shows the diffuse reflectance and the absorption spectra of $RE_{1.8}Sr_{0.2}CuO_{4\pm\delta}$ (RE=La, Pr, Nd) respectively. The absorption spectrum F(R) can be obtained from the diffuse reflectance (R) by using the Kubelka–Munk function [23]:

$$F(R) = \frac{(1-R)^2}{2R} = \frac{K}{S} \quad (2)$$

Where: S, K and R are the scattering coefficient, the absorption coefficient and the diffuse reflectance respectively.

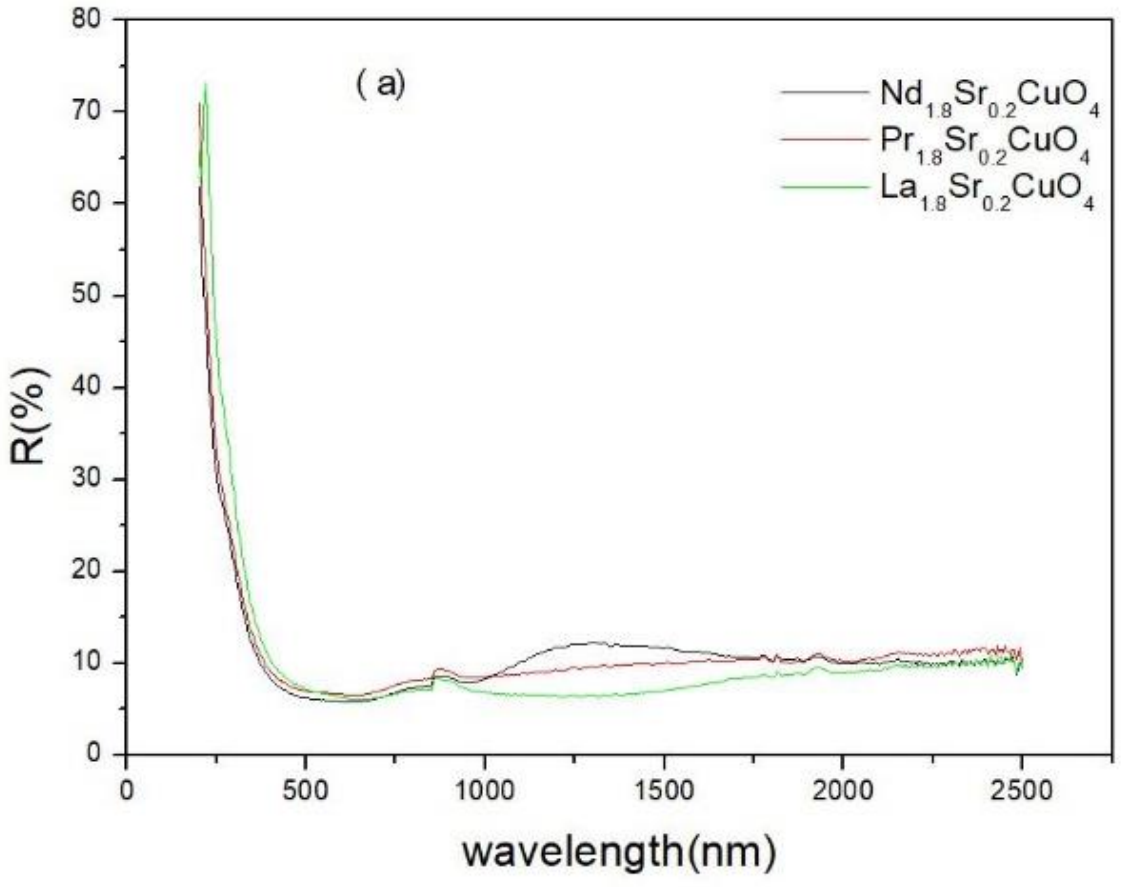

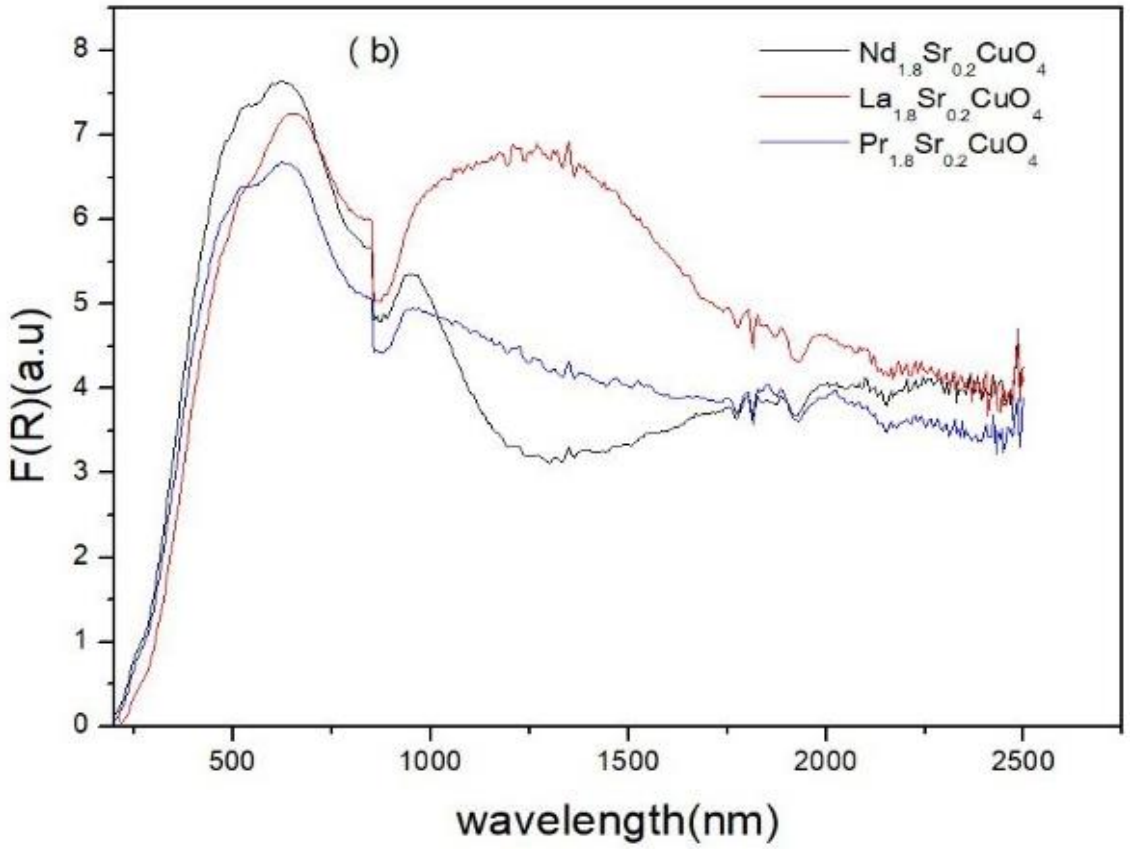

Figure 3. (a) Diffuse reflectance and **(b)** absorption spectra of $RE_{1.8}Sr_{0.2}CuO_4$ (RE=La, Pr, Nd)

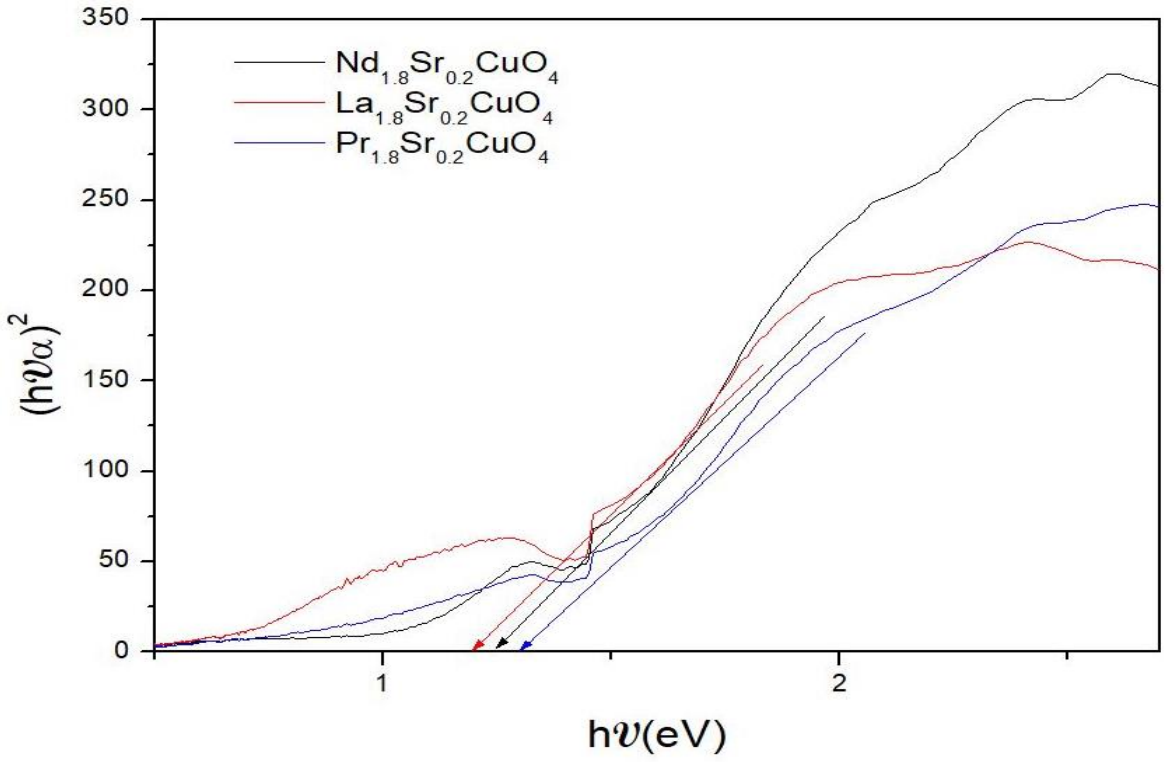

Figure 4. A Plot of $(\alpha h\nu)^2$ versus photon energy ($h\nu$) of the calculation of band gap of $RE_{1.8}Sr_{0.2}CuO_{4\pm\delta}$ (RE=La, Pr, Nd).

Clearly, all of the samples exhibit a broad absorption. The absorption spectrum have been firstly recorded under UV excitation between 300 nm and 750 nm. The absorption band located between 350 and 450 nm could be clearly observed due to the charge transfer transitions of Cu–O and RE–O and the strong d–d electron transitions [24]. In order to determinate the optical band gap energy, the Tauc plot method [25] have been used:

$(\alpha h\nu)^2 = C_1(h\nu - Eg)$ (3)

and $\alpha = F(R)$ (4)

Where hν is the energy of photon and C1 is the constant of proportionality.

The optical band gap energies were estimated by extrapolating of the straight line portion of the $(\alpha h\nu)^2$ as function of photon energy (E=hν) plot until null absorption (Figure 4). Thus, the optical band gap energies of the title compounds are estimated to 1.30 eV for $Pr_{1.8}Sr_{0.2}CuO_{4\pm\delta}$, 1.24 eV for $Nd_{1.8}Sr_{0.2}CuO_{4\pm\delta}$ and 1.19 eV for $La_{1.8}Sr_{0.2}CuO_{4\pm\delta}$. Four observations can be written:

- According to the optical band gap values of $RE_{1.8}Sr_{0.2}CuO_{4\pm\delta}$ (RE=La, Pr, Nd), these materials may be classed as semi-conductors.
- The band gap value of two samples ($Pr_{1.8}Sr_{0.2}CuO_{4\pm\delta}$ and $Nd_{1.8}Sr_{0.2}CuO_{4\pm\delta}$) are between 1.23 eV and 2.1 eV. Thus these samples may be used in photocatalytic reactions or as photocathode in the photo-electrochemical decomposing of water.
- The band gap energy decrease with the increase in the rare earth ionic radii which was mentioned in the introduction.
- The comparison between the gap energy of undoped rare earth copper oxides (RE_2CuO_4, RE=La, Pr, Nd) which were 1.24 eV, 0.79 eV and 1.06 eV respectively and the obtained value 1.19 eV, 1.30 eV, 1.24 eV of $La_{1.8}Sr_{0.2}CuO_{4\pm\delta}$, $Pr_{1.8}Sr_{0.2}CuO_{4\pm\delta}$ and $Nd_{1.8}Sr_{0.2}CuO_{4\pm\delta}$ respectively. The variation (from undoped to doped) is not monotonic and this is due may be to the effect of microstructure and grain size.

3.4. Dielectric study

The dielectric study has been carried out for the three cuprates in the 250 to 450°C temperature range. The complex permittivity (ε*), the dielectric constant (ε′), the dielectric loss (ε′′) and the conduction loss (tan δ) were deduced from Z' and Z" the real part and the imaginary part of impedance respectively [26]:

$$\varepsilon^* = \varepsilon' - j\,\varepsilon'' = \frac{1}{j\omega C_0(Z' + jZ'')} \quad (5)$$

Where:

$$\varepsilon' = -\frac{Z''}{\omega C_0(Z'^2 + Z''^2)} \quad (6) \text{ and } \varepsilon'' = -\frac{Z'}{\omega C_0(Z'^2 + Z''^2)} \quad (7)$$

And

$$\tan\delta = \frac{\varepsilon''}{\varepsilon'} \quad (8)$$

where. $C_0 = \frac{\varepsilon_0 A}{e}$ is the capacitance of the empty cell (ε_0 is the permittivity of the vacuum 8.854 10^{-12} Fm^{-1}, A is the cross sectional area of the flat surface of the pellet and *e* is its thickness).

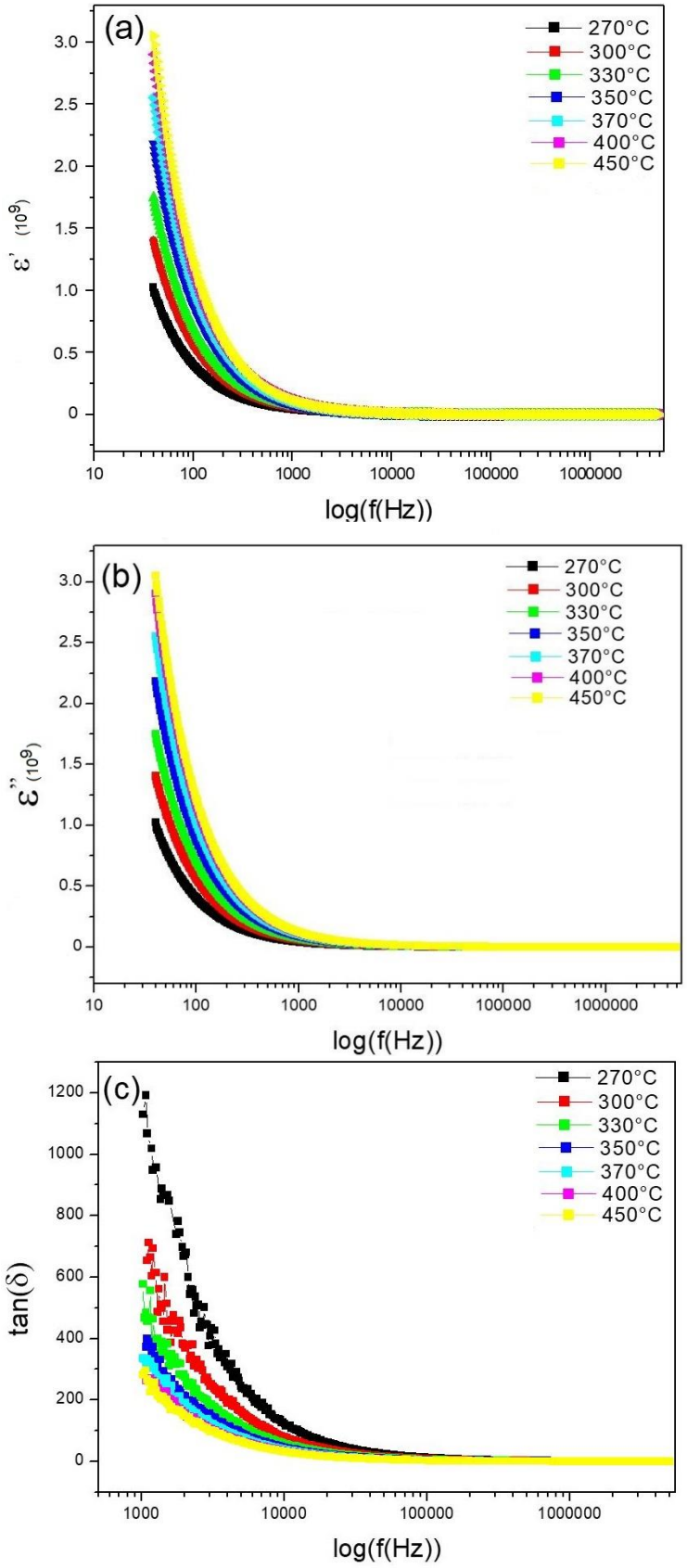

Figure 5. The frequency dependence curves of **(a)** Dielectric constant ε' **(b)** Conduction loss ε'' and **(c)** dielectric loss of $La_{1.8}Sr_{0.2}CuO_{4\pm\delta}$.

The variation of dielectric constant ε'(ω), the conduction loss ε"(ω) and the tangent loss for the cuprate $La_{1.8}Sr_{0.2}CuO_{4\pm\delta}$ at various temperatures as a function of frequency are illustrated in Figure 5.

It can be observed that the dielectric constant ε'(ω) increases with the increase of the temperature and decrease with the increase of the frequency (Figure 5.a). At low frequency, ε'(ω) is very high (≈ 3.10^9), then it tends to be zero at high frequency.

The variation of the conduction loss ε"(ω) with the frequency (Figure 5.b) shows that at low frequency the conduction loss is predominate and it decreases at high frequency. In general, when a dielectric material is subjected to the alternating current voltage, the electric energy is absorbed by the material and is dissipated in the form of heat because of friction [13]. The dependence of this conduction loss to the frequency may be due to the polarization [29] or to the residual ohmic conduction of the dielectric material [30].

The variation of the dielectric loss (Tan(δ)) with the frequency is shown in Figure 5.c. It can be seen that the dielectric loss has a high value at law frequency. On the other side, at high frequency it tends to be zero. This behavior can be explained as: at low frequency, there is a phase shift between the polarization vector and the electric field [31]. At high frequency, the period of electric field becoming small compared to the relaxation time of the permanent dipoles, the orientation of the latter is no longer influenced by the electric field and remains random [13, 31-33].

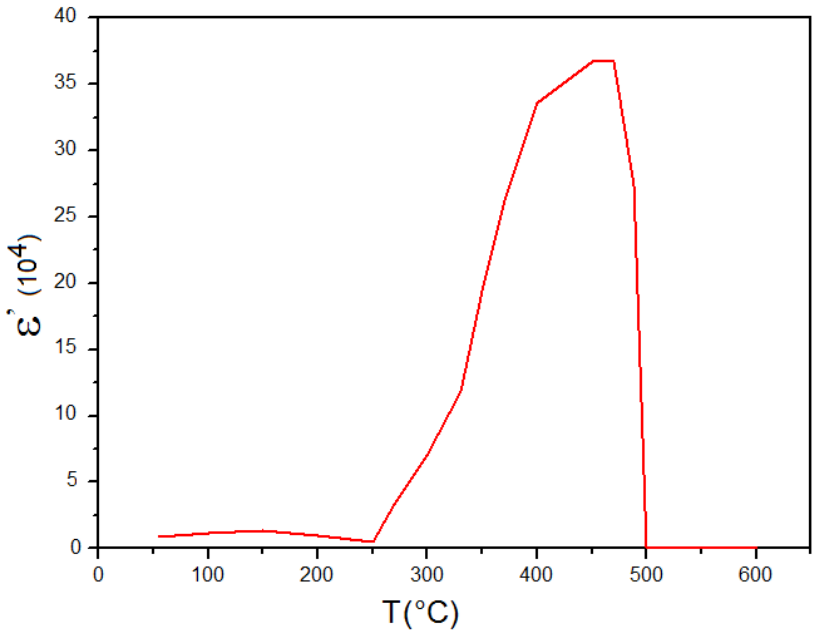

Figure 6. The temperature dependence curves of dielectric constant ε' of $La_{1.8}Sr_{0.2}CuO_{4\pm\delta}$.

The dielectric constant depends also on the structure which in turn depends on the temperature. Figure 6 shows the variation of ε'(ω) at various temperature. We observe the phase change of $La_{1.8}Sr_{0.2}CuO_{4\pm\delta}$ in 400 °C which confirms the Figure 5.a. Wherein, we notice a remarkable increase in the ε'(ω) resulting from the phase change. In fact, with the increase of the temperature, oxygen vacancies increase due to the increase of space charge polarization. As a result, the dielectric constant increases [30].

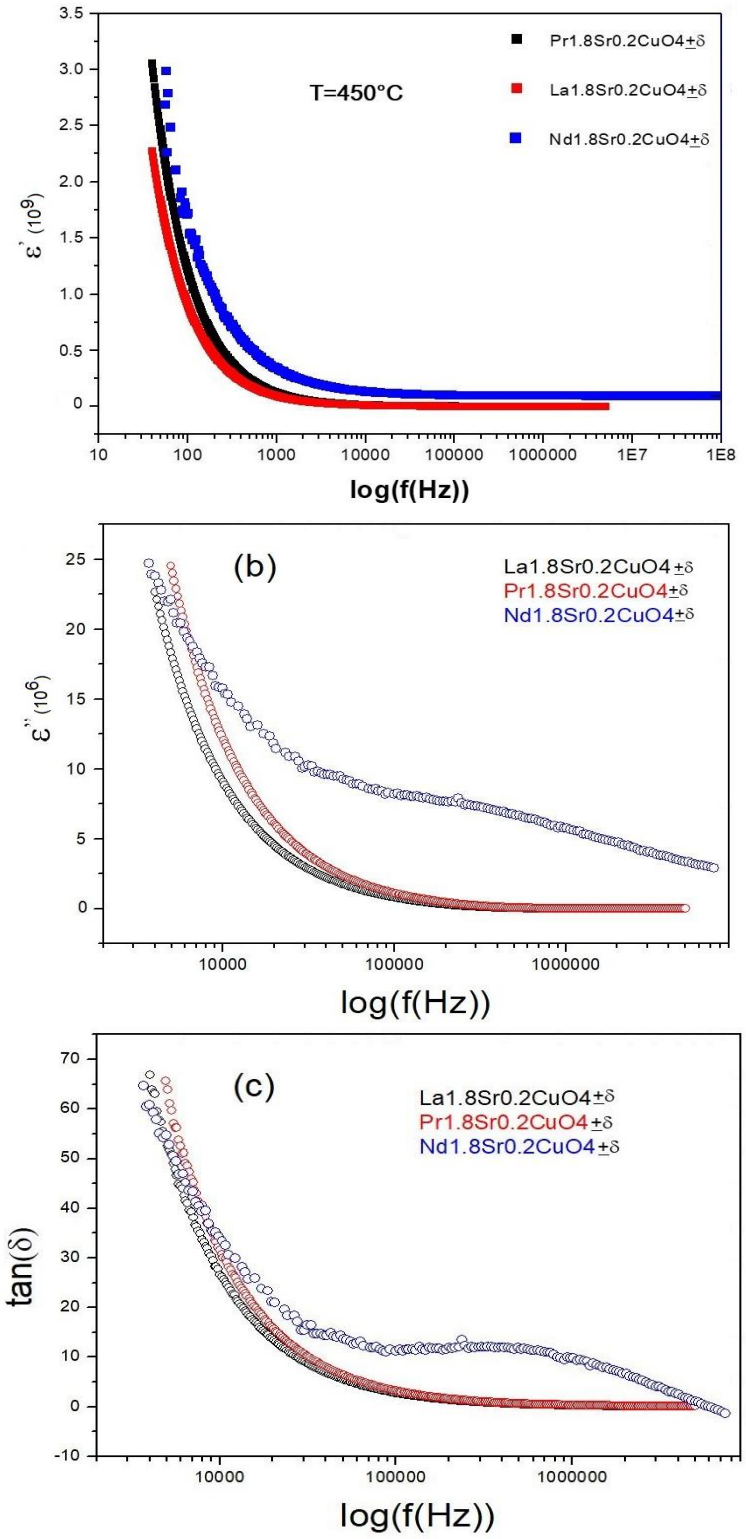

Figure 7. The frequency dependence curves of Dielectric constant ε', conduction loss ε'' and dielectric loss of $RE_{1.8}Sr_{0.2}CuO_{4\pm\delta}$ at T=450°C (RE= La, Pr, Nd)

Figure 7.a shows the comparison between constant loss ε'(ω) of the three cuprates at 450 °C. For $La_{1.8}Sr_{0.2}CuO_4$ and $Pr_{1.8}Sr_{0.2}CuO_{4\pm\delta}$, the values of ε'(ω) are very high and close. At low frequency, they

have an average value of about 3.10^9. Consequently, the two materials $La_{1.8}Sr_{0.2}CuO_{4\pm\delta}$ and $Pr_{1.8}Sr_{0.2}CuO_{4\pm\delta}$ have a very large capacitive effect and they may be classified as insulators materials. In the other hand, at high frequency, ε'(ω) is very low which implies that $La_{1.8}Sr_{0.2}CuO_{4\pm\delta}$ and $Pr_{1.8}Sr_{0.2}CuO_{4\pm\delta}$ have a conductive effect. For the material $Nd_{1.8}Sr_{0.2}CuO_{4\pm\delta,}$ it has a very small value ε'(ω) at low frequency and it can be classified as a bad insulator.

Figure 7.b shows the variation of ε"(ω) as function of the frequency for the oxides $RE_{1.8}Sr_{0.2}CuO_{4\pm\delta}$ (RE=La, Pr, Nd). At low frequency, $La_{1.8}Sr_{0.2}CuO_{4\pm\delta}$ and $Pr_{1.8}Sr_{0.2}CuO_{4\pm\delta}$ have high values of ε"(ω) ≈ 25.10^6. This behavior may be indicate that at low frequency $La_{1.8}Sr_{0.2}CuO_{4\pm\delta}$ and $Pr_{1.8}Sr_{0.2}CuO_{4\pm\delta}$ are able to absorb a lot the electric energy. However, $Nd_{1.8}Sr_{0.2}CuO_{4\pm\delta}$ does not have a great conduction loss throughout the range of frequency.

Figure 7.c shows the comparison of the dielectric loss. The two materials $La_{1.8}Sr_{0.2}CuO_{4\pm\delta}$ and $Pr_{1.8}Sr_{0.2}CuO_{4\pm\delta}$ have high dielectric loss ≈ 65 compared to $Nd_{1.8}Sr_{0.2}CuO_{4\pm\delta}$ which has a very low value ≈ 0.65.

3.5. Modulus study

The dielectric study shows that the presence of the dielectric loss is due to the conductivity of the material. In order to explore this phenomenon in detail, the electric modulus formalism M* was used. The electric modulus M* is the reciprocal of the permittivity ε*, it is used for studying the space charge relaxation phenomena [30] and to analyze ionic conductivities.

$$M^* = M' + jM'' = \frac{1}{\varepsilon^*} = jC_0\omega Z^* \quad (9)$$

Where:

$$M' = \omega C_0 Z'' \quad (10)$$

And

$$M'' = \omega C_0 Z' \quad (11)$$

Where C_0 is the capacitance of the empty cell.

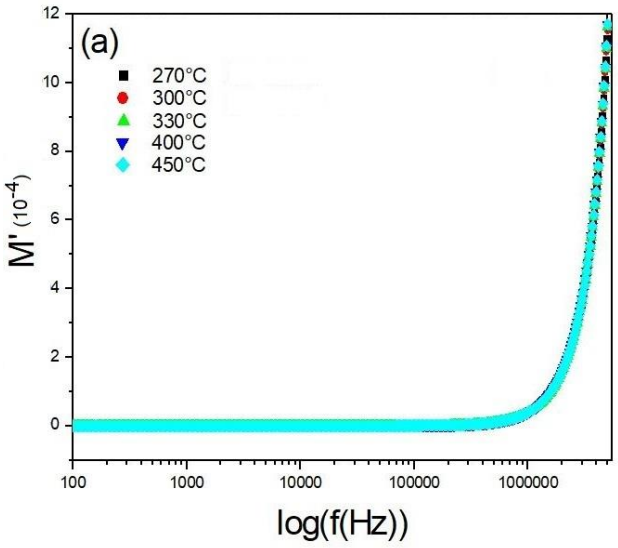

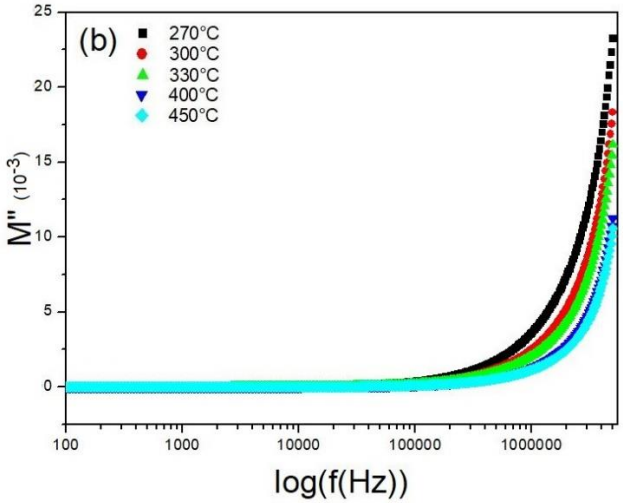

Figure 8. The frequency dependence of M' (a) and M" (b) for $La_{1.8}Sr_{0.2}CuO_{4\pm\delta}$ oxide at different temperature.

The frequency dependence of the real M' and the imaginary M" parts of the electric modulus for $La_{1.8}Sr_{0.2}CuO_{4\pm\delta}$ oxide at different temperatures from 270 to 450°C are shown in Figure 8. The value of M' increases with the increase of the frequency (Figure 8.a). M' tend to be zero at low frequency and this may be due to the absence of electrode polarization phenomena [34]. M' exhibits an increasing trend with the increase of the frequency but it stills has law value (M'≈0.0012) at high frequency. Figure 8.a shows a continuous dispersion with the increase of the frequency at all the temperatures attributed to the conduction phenomena, it may be due to short-range mobility of charge carriers [35].

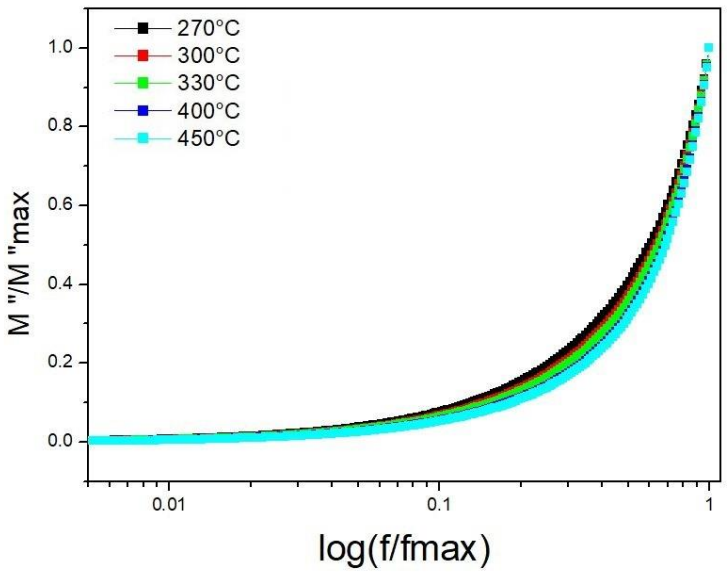

Figure 9. Curves M''/M''$_{max}$ versus log (f/f_{max}) for $La_{1.8}Sr_{0.2}CuO_{4\pm\delta}$ oxide at different temperatures.

The variation of the imaginary part of the modulus M" as function of the frequency is visualized in Figure 8.b. The low value of M" at low frequency suggests that the ions can move for long distances whereas, at high frequency, the low value of M" favors the confinement of ions in their potentials wells [35]. In addition, M" moves to higher relaxation frequencies with the increase of the temperature. This

behavior suggests that the dielectric relaxation is thermally activated in which the hopping mechanism of the charges carriers dominate intrinsically [34].

The normalized plots of M"/M"$_{max}$ versus f/f$_{max}$ at different temperatures for the different oxides $RE_{1.8}Sr_{0.2}CuO_{4\pm\delta}$ (RE=La, Pr, Nd) are shown in Figure 9. The plots overlaps on a single curve at different temperatures. This results indicates that the dielectric relaxation for all the samples is independent to the temperature [36].

Figure 10 presents the frequency dependence of the real M' and the imaginary M" parts of the electric modulus for $Nd_{1.8}Sr_{0.2}CuO_{4\pm\delta}$ oxide at different temperatures from 270 to 450°C.

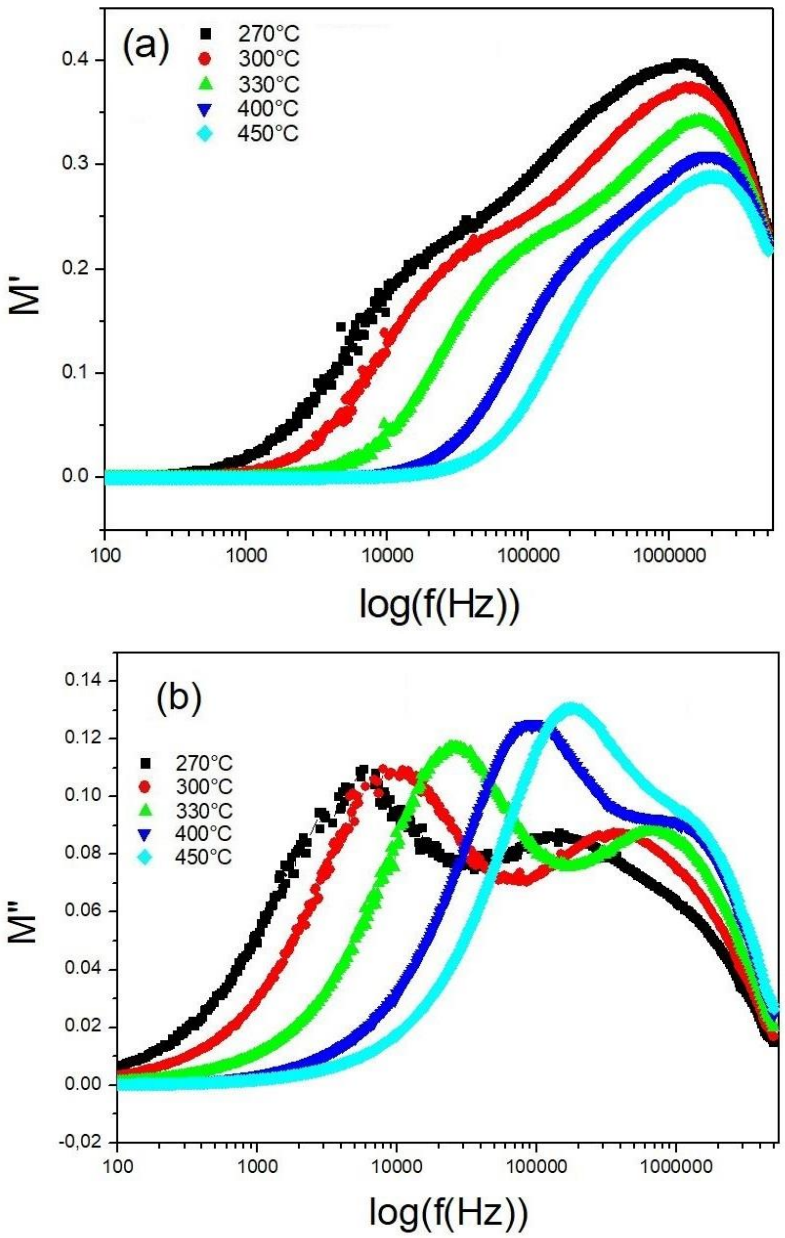

Figure 10. The frequency dependence of M' (a) and M" (b) for $Nd_{1.8}Sr_{0.2}CuO_{4\pm\delta}$ oxide at different temperature.

The value of M' increases with the increase of the frequency (Figure 10.a) and decreases with the increase of the temperature. All curves reach the same value at high frequency M_∞ (M_∞ is the asymptotic value of M' at high frequency). The nature of the variation indicates that the electrical properties of the materials is due to the bulk [32].

The imaginary part of the electric modulus for $Nd_{1.8}Sr_{0.2}CuO_{4\pm\delta}$ oxide is shown in the Figure 10.b. All samples show two peaks of relaxation. The two peaks are observed in low and middle frequency. The shift of the peaks implies that when the temperature increases, the relaxation time decreases. This distribution of relaxation times is generally attributed to the environmental difference surrounding the different ions in the cuprates [35].

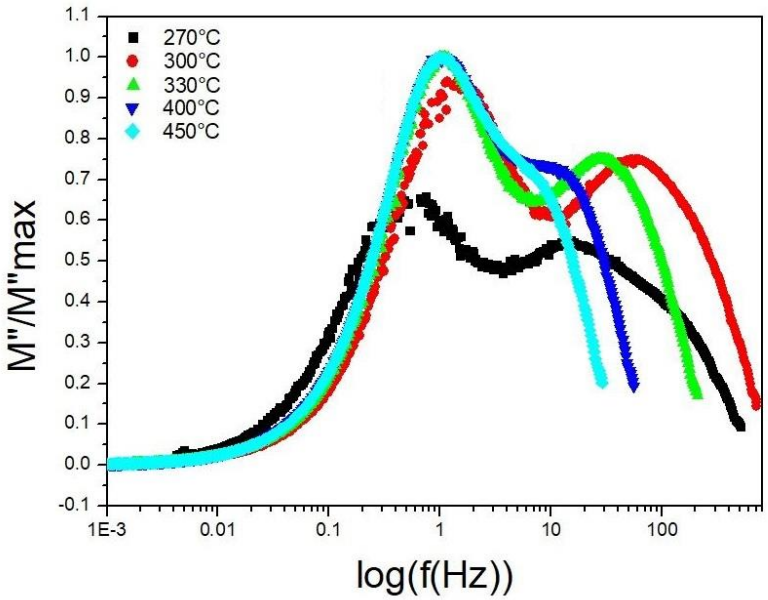

Figure 11. Curves M''/M''max versus log (f/fmax) for $Nd_{1.8}Sr_{0.2}CuO_{4\pm\delta}$ oxide at different temperatures.

Figure 11 shows the normalized plot of M"/M"$_{max}$ versus f/f_{max} for $Nd_{1.8}Sr_{0.2}CuO_{4\pm\delta}$ oxide at different temperatures. All the curves have tow peaks, the first peak at low frequency indicates that there is a relaxation of grain boundaries, while the second one at high frequency proves the grain relaxation [33]. The absence of overlap of all the curves on a single master indicate that the dielectric relaxation is thermally activated.

4. CONCLUSION

Three rare earth copper oxides samples $RE_{1.8}Sr_{0.2}CuO_4$ (RE=La, Pr, Nd) have been prepared by using the solid state reaction. The title compounds crystallize in tetragonal system, space group *I4/mmm*. The optical band gap of $Pr_{1.8}Sr_{0.2}CuO_{4\pm\delta}$, $Nd_{1.8}Sr_{0.2}CuO_{4\pm\delta}$ and $La_{1.8}Sr_{0.2}CuO_{4\pm\delta}$ are estimated to 1.30 eV, 1.24 eV and 1.20 eV respectively. For the dielectric properties study, $Pr_{1.8}Sr_{0.2}CuO_{4\pm\delta}$ and

$La_{1.8}Sr_{0.2}CuO_{4\pm\delta}$ have, at low frequency, a very high value of ε'(ω) (≈3.10^9) and a tanδ (≈70) compared to $Nd_{1.8}Sr_{0.2}CuO_{4\pm\delta}$ which has a low value of ε'(ω) (≈800) and low tanδ (≈0.6). The observed double peaks in the complex modulus plots confirmed the contribution of bulk and grain boundary effects to the electrical properties of the compounds. The dielectric relaxation is thermally activated in $Nd_{1.8}Sr_{0.2}CuO_{4\pm\delta}$, while the thermal factor does not influence the dielectric relaxation of $Pr_{1.8}Sr_{0.2}CuO_{4\pm\delta}$ and $La_{1.8}Sr_{0.2}CuO_{4\pm\delta}$.

ACKNOWLEDGMENT
The authors extend their appreciation to the Deanship of Scientific Research at King Khalid University for funding this work through research groups program under grant number R.G.P.2/46/40. The authors extend also their appreciation to the Tunisian Ministry of Higher Education and Scientific Research for funding this work through research groups program.

References

1. J.A. Kilner, M. Burriel, *Annu. Rev. Mater. Res.*, 44 (2014) 365.
2. W. Paulus, G. Heger, P. Rudolf, R. Schöllhorn, *Physica C*, 235-240 (1994) 861.
3. Y. Tokura, H. Takagi, S. Uchida, *Nature,* 337 (1989) 345.
4. W. Paulus, A. Cousson, G. Dhalenne, J. Berthon, A. Revcolevschi, S. Hosoya, W. Treutmann, G. Heger, R. Le Toquin, *Solid State Sci.*, 4 (2002) 565.
5. J.G. Bednorz, K.A. Miiller, *Physica B,* 64 (1986) 189.
6. R.A. Fisher, J.E. Gordon, N. E. Phillips, *Annu. Rev. Phys. Chem.*, 47 (1996) 283.
7. A. Nemudry, P. Rudolf, R. Schöllhorn, *Solid State Ionics,* 109 (1998) 213.
8. D. Chen, C. Lin, A. Maljuk, F. Zhou. Growth and characterization of bulk superconductor material, Springer International Publishing (2016) Switzerland.
9. H. Kamimura, H. Ushio, S. Matsuno, T. Hamada. Theory of Copper Oxide Superconductors, Springer (2005) Berlin, Germany.
10. P.H. Salame, O. Prakash, A.R. Kulkarni, *Ceram. Int.*, 42 (2016) 13207.
11. K. Iwauchi, *Phys. Status Solidi A,* 130 (1992) 219.
12. P.H. Salame, R. Drai, O. Prakash, A.R. Kulkarni, *Ceram. Int.,* 40 (2014) 4491.
13. V. Anbarasu, A. Manigandan, K. Sivakumar, *J. Modern physics, 1* (2010) 93.
14. P.H. Salame, O. Prakash, A.R. Kulkarni, *J. Am. Ceram. Soc.*, 96 (2013) 2184.
15. J.B. Shi, Y. Hsu, C.T. Lin, *Physica C*, 29 (1998) 272.
16. P.H. Salame, O. Prakash, A.R. Kulkarni, *Ceram. Int.,* 43 (2017) 14101.
17. M. Enhessari, M. Shaterian, M.J. Esfahani, M.N. Motaharian, *Mater. Sci. Semicond. Process.,* 16 (2013) 1517.
18. D.V. Dharmadhikari, A.A. Athawle, *Mateials Sciences and engineering B*, 229 (2018) 70.
19. Y. Li, J. Huang, L. Cao, J. Wu, J. Fei, *Materials Characterization,* 64 (2012) 36.
20. M. Sukumar, L.J. Kennedy, J.J. Vijaya, B. Al-Najar, M. Bououdina, *Ceram. Int.,* 44 (2018) 18113.
21. M. Sukumar, L.J. Kennedy, J.J. Vijaya, B. Al-Najar, M. Bououdina, *J. Magn. Magn. Mater.,* 465 (2018) 48.
22. U. Holzwarth, N. Gibson, *Nat. Nanotechnol.,* 6 (2011) 534.
23. J. Tauc, R. Grigorovici, A. Vancu, *Phys. Status Solidi B*, 15 (1966) 627.
24. S. Shanavas, A. Priyadharsan, V. Vasanthakumar, A. Arunkumar, P.M. Anbarasan, S. Bharathkumar, *J. Photochem. Photobiol., A,*188 (2007) 185.
25. S. Adachi, *Phys. Rev. B: Condens. Matter.,* 43(1991) 12316.
26. A.M. George, I.K. Gopalakrishnan, M.D. Karkhanavala, *Mater. Res. Bull.*, 9 (1974) 721.
27. W. Hzez, A. Benali, H. Rahmouni, E. Dhahri, K. Khirouni, B.F.O. Costa, *J. Phys. Chem. Solids,*117

(2018) 1.
28. P. Salame, R. Drai, O. Prakash, A.R. Kulkarni, *Ceram. Int.,* 40 (2014) 4491.
29. S.G. Kakade, R.C. Kambale, Y.D. Kolekar, C.V. Ramana, *J. Phys. Chem. Solids,* 98 (2016) 20.
30. P.H. Salame, O. Prakash, A.R. kulkarni, *Ceram. Int.,* 42 (2016) 13207.
31. H.M. Li, C.H. Ra, G. Zhang, W.J. Yoo, *J. Korean Phys. Soc.,* 54 (2009) 1096.
32. A. Tabib, N. Sdiri, H. Elhouichet, M. Férid, *J. Alloys Compd.*, 622 (2015) 687.
33. A. Langar, N. Sdiri, H. Elhouichet, M. Férid, *J. Alloys Compd.,* 590 (2014) 380.
34. S. Das, A. Dutta, B. Ghosh, S.Banerje, T. P. Sinha, *J. Phys. Chem. Solids.,* 75 (2014) 1245.
35. T.B. Adams, D.C. Sinclair, A.R. West, *Phys. Rev. B: Condens. Matter.*, 73 (2016) 094124.
36. J.T.S. Irvine, D.C. Sinclair, A.R. West, *Adv. Mater.*, 2 (1990) 132.